Room temperature ferromagnetism in InSb-Mn nanowires

Katarzyna E. Hnida[1,], Antoni Żywczak[1], Marcin Sikora[1], Marianna Marciszko[1], Marek Przybylski[1,2]*

[1]AGH University of Science and Technology, Academic Centre for Materials and Nanotechnology, A. Mickiewicza 30, 30-059 Krakow, Poland

[2]AGH University of Science and Technology, Faculty of Physics and Applied Computer Science, A. Mickiewicza 30, 30-059 Krakow, Poland

Corresponding Author

*K.E. Hnida, e-mail: khnida@agh.edu.pl, katarzyna.hnida@gmail.com

AGH University of Science and Technology, Academic Centre for Materials and Nanotechnology, av. A. Mickiewicza 30, 30-059 Krakow, Poland; Tel: + 48 12 617 53 09

InSb-Mn nanowires preparation and characterization

The anodic aluminum oxide (AAO) templates were synthesized using conditions described previously from the electropolished Al foil by a two-step anodization.[1] The resulting templates had a pore diameter of about 55-60 nm. The electrodeposition experiments were carried out using the potentiostat/galvanostat BioLogic SP300 with a three-electrode setup with Ag/AgCl (3M NaCl) electrode as a reference electrode (RE), Pt wire as a counter electrode and AAO covered with the Au film as a working electrode (WR). For electrodeposition of Mn-doped InSb nanowires protocol for InSb NW synthesis reported previously by Hnida et al. was employed.[2] The electrolyte used for the electrodeposition of Mn-doped InSb NW was composed of 0.06 M $InCl_3$, 0.04 M $SbCl_3$, 0.2 M citric acid, 0.17 M sodium citrate and appropriate amount of $MnCl_2 \cdot 4H_2O$ (0.003-0.3M). All electrolyte component were analytically grade. The structural and morphological characterizations of ternary nanowires were performed with a scanning electron microscope (FEI Versa 3D). To determine In/Sb ratio and estimate the % at. Mn introduced into nanowires energy-dispersive X-ray spectroscopy (EDX) was used. To confirm the presence of Mn and to verify its local atomic environment XAFS spectra of free-standing InSb-Mn nanowire arrays were collected at PEEM/XAS beamline of Solaris (National Synchrotron Radiation Centre, Poland). Measurements were performed at room temperature in the photon energy range of 400-800 eV using total electron yield detection. To establish whether nanowires contain MnSb/Mn_2Sb phases or Mn clusters X-ray diffraction analysis (XRD) were performed at Panalytical Empyrean diffractometer (Cu K_α = 1.5406 Å). Magnetic properties of the nanowires were probed prior to removing them from magnetically inert oxide template. Magnetization measurements were probed using LakeShore 7407 magnetometer (VSM) under applied magnetic field up to 0.5T in the

temperature range from 100K to 450K. Results were scaled to the volume of each sample in order to track the effective magnetization evolution vs. Mn content.

Magnetic response of InSb-Mn nanowires containing 2.5% at. Mn

Figure S1 extends the data shown in Figure 2A and presents magnetic response of the sample containing 2.5% at. Mn (highest concentration of dopant possible to incorporate during electrosyntesis) at 100K and 300K. Both, open loops and linear dependence of *M(B)* at higher fields that decreases with increasing T, confirm mixed nature of obtained nanowires (ferromagnetic with a clear admixture of paramagnetic/antiferromagnetic contribution).

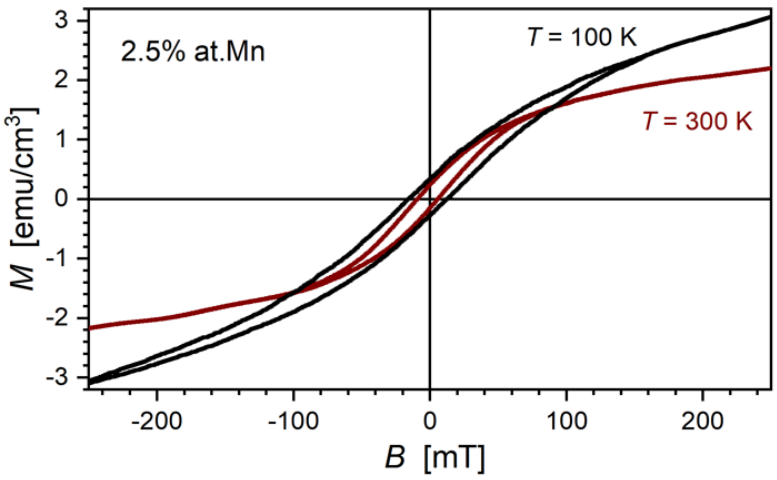

Figure S1. Comparison of hysteresis loops registered at 100K and 300K for nanowires containing 2.5% at. Mn.

Binomial distribution of the doping dependence of magnetization

Magnetic nature of the nanowires depends on population of dimers, trimmers etc., as shown in Figure 2B. Probability of finding certain number of Mn ions in the next neighbour shell around

given Mn ion residing in InSb lattice at given doping level has been determined using bimodal distribution:

$$f(n,p,k) = \binom{n}{k} p^k (1-p)^{n-k} \quad (1)$$

where:

p – concentration of Mn dopants,

$n = 4$,

k – expected number of neighbours.

At low doping level the events with $k > 2$ are negligible small. *M(x)* dependences shown in Figure 2B were obtained assuming two scenarios:

1. Week magnetic response of paramagnetic single Mn ions ($k = 0$), 5x stronger response – mixed anti-/ferromagnetic – of Mn_2 dimers ($k = 1$) and 25x stronger response – mixed ferri/ferromagnetic – of Mn_3 trimers.

2. Strong tendency to antiferromagnetic dimerization above 1% at. Mn. Here the identical parameters were used as in scenario 1, but paramagnetic ions ($k = 0$) at $p > 0.01$ were forced to form dimer with other paramagnetic ion. Effective susceptibility of such dimer was assumed negligibly small (equal to zero). In other words, the fraction of paramagnetic ions increases according to binomial distribution up to 1% at. Mn, then it decreases in the concentration range up to approx. 2% at. Mn. The existence of dimers and trimmers is allowed only at higher concentration of Mn atoms. The fraction of the former being given by *f(4,p,1) + 0.5f(4,p,0)*.

Temperature dependence of magnetization of InSb-Mn nanowires containing 2.5% at. Mn

In order to better understand the magnetic properties of InSb-Mn nanowires doped with 2.5% at. Mn, an extended version of *M(T)* graph (with respect to the Figure 2C) is presented in Figure

S2. The figure compares three magnetics models which can be used to characterize nanostructures doped with manganese.

Temperature dependence of magnetization of InSb-Mn NWs containing 2.5% at. Mn (Figure S2) can be explained by presence of two coexisting magnetic phases. The first phase yields a antiferromagnetic contribution (M_{AF}), the second phase is attributable to (ferro/ferri)magnetic phase (M_{FM}). The total magnetization can be described as a sum of those contributions – equation (2)[3].

$$M(T) = M_{AF}(T) + M_{FM}(T) \qquad (2)$$

where:

$M_{AF}(T)$ – magnetization of antiferromagnetic phase,

$M_{FM}(T)$ - magnetization of (ferro/ferri)magnetic phase.

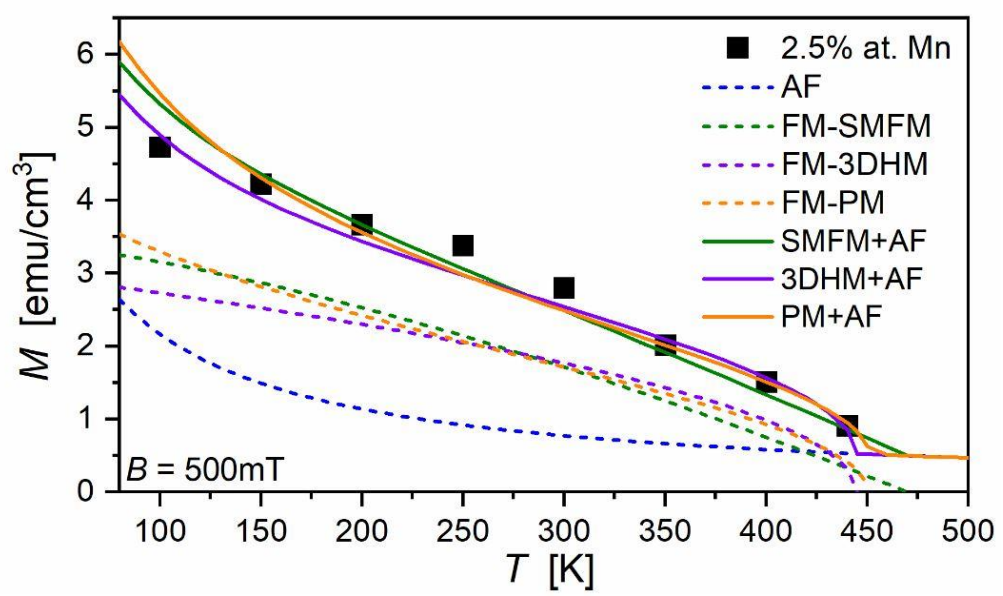

Figure S2. Temperature dependence of magnetization at B = 500mT for NWs with 2.5% at. Mn. Dashed lines show ferromagnetic models such as: 3D Heisenberg model (FM-3DHM – violet), polaronic model (FM-PM – orange), static mean field model (FM-SMFM – olive) and antiferromagnetic component (AF – blue). Solid lines present the results of dual phase (AF + FM)

approximation using corresponding models (3DHM+AF – violet line, polaronic model (PM – orange line), static mean field model (SMFM – olive line).

The expression for the temperature variation of magnetization of antiferromagnetic phase is given by Curie-Weiss law (3) (blue dash line in Figure S2):

$$M_{AF}(T) = \frac{C}{T+\theta} \qquad (3)$$

where:

C – magnetization of antiferromagnetic phase at 0 K [emu/cm^3],

θ – the critical temperature [K].

The magnetization vs temperature of ferro/ferri magnetic phase in ferromagnetic semiconductors can be explained on the basis of three different models:

a) 3D Heisenberg (3DHM) (violet dashed line in Figure S2; annotation: FM-3DHM)[4]:

$$M_{FM}(T) = M_0 * (1 - \frac{T}{T_C})^{0.5} \qquad (4)$$

where:

M_0 - magnetization of ferro/ferri magnetic phase at 0 K [emu/cm^3],

T_C – Curie temperature [K].

b) polaronic (PM) (orange dashed line in Figure S2; annotation: FM-PM)[5]:

$$M_{FM}(T) = M_0 * (0.86 + A * \ln(\frac{T_C}{T}))^{0.5} \qquad (5)$$

where:

A – dimensionless parameter.

c) static mean field (SMFM) (olive dashed line in Figure S2; annotation: FM-SMFM)[5]:

$$M_{FM}(T) = M_0 * (1 - (\frac{T}{T_C})^{1.5}) \qquad (6)$$

Although, the different models to explain the $M(T)$ dependence in ferromagnetic semiconductors were proposed, it is not possible to judge, within achieved accuracy, which magnetic coupling scheme is predominant.

REFERENCES

(1) Hnida, K. E.; Żywczak, A.; Gajewska, M.; Marciszko, M.; Sulka, G. D.; Przybylski, M. Tuning the Magnetic Properties of Multilayered CoPt-Pt Nanowires via Thickness of Magnetic Segments. *Electrochimica Acta* **2016**, *205*, 29–37. https://doi.org/10.1016/j.electacta.2016.04.076.

(2) Hnida, K. E.; Bäβler, S.; Akinsinde, L.; Gooth, J.; Nielsch, K.; Socha, R. P.; Łaszcz, A.; Czerwinski, A.; Sulka, G. D. Tuning the Polarity of Charge Transport in InSb Nanowires via Heat Treatment. *Nanotechnology* **2015**, *26* (28), 285701. https://doi.org/10.1088/0957-4484/26/28/285701.

(3) Kochura, A. V.; Aronzon, B. A.; Lisunov, K. G.; Lashkul, A. V.; Sidorenko, A. A.; De Renzi, R.; Marenkin, S. F.; Alam, M.; Kuzmenko, A. P.; Lähderanta, E. Structural and Magnetic Properties of $In_{1-x}Mn_xSb$: Effect of Mn Complexes and MnSb Nanoprecipitates. *Journal of Applied Physics* **2013**, *113* (8), 083905. https://doi.org/10.1063/1.4792652.

(4) Das Sarma, S.; Hwang, E. H.; Kaminski, A. Temperature-Dependent Magnetization in Diluted Magnetic Semiconductors. *Phys. Rev. B* **2003**, *67* (15), 155201. https://doi.org/10.1103/PhysRevB.67.155201.

(5) Kaminski, A.; Das Sarma, S. Polaron Percolation in Diluted Magnetic Semiconductors. *Phys. Rev. Lett.* **2002**, *88* (24), 247202. https://doi.org/10.1103/PhysRevLett.88.247202.